*Materials Research*. 2023; 26: e20220390
DOI: https://doi.org/10.1590/1980-5373-MR-2022-0390

# Processing Biodegradable Blends of Hemicellulose with Polyhydroxybutyrate and Poly (Lactic Acid)

*Ívia Maria Lourenço Mendes*[a], *Michaella Socorro Bruce Fialho*[b*], *Rosineide Miranda Leão*[c], *Edgar A. Silveira*[b], *Sandra Maria da Luz*[a,b]

[a]*Universidade de Brasília, Faculdade de Gama, Laboratório de Tecnologias de Biomassa, Brasília, DF, Brasil.*
[b]*Universidade de Brasília, Programa de Pós-Graduação em Ciências Mecânicas, Brasília, DF, Brasil.*
[c]*Universidade Paulista, Instituto de Ciências Exatas, Brasília, DF, Brasil.*

Received: September 01, 2022; Revised: January 16, 2023; Accepted: March 23, 2023

The bottleneck of hemicellulose as a bio-based material is its processability and property drawbacks (softening and hydrophilicity). Thus, mixing other biopolymers can be an alternative. This article proposes blending hemicellulose (10−50 wt%) with polyhydroxybutyrate (PHB) and poly (lactic acid) (PLA), using acetic acid and chloroform as casting solvents to improve its processability and thermal properties. The materials were thermally (TGA – thermogravimetric analysis), chemically (FTIR – Fourier transformer infrared) and morphologically (SEM – scanning electron microscopy) characterized. Finally, a multicriteria decision analysis (MCDA) evaluated the materials' properties to identify the optimum combination (casting solvent, biopolymer and hemicelluloses proportion) for producing an optimal blend. The MCDA established that the blend of hemicellulose:PHB (10:90 wt/wt) produced with acetic acid was optimum considering melting temperature and the crystallinity criteria. Moreover, higher hemicellulose concentration in the blends decreased the MCDA success rate, indicating the worst properties. PLA blends showed a higher degradation temperature than PHB. The PHB blends produced with acetic acid demonstrated improved properties when compared to chloroform, revealing its potential as a solvent.

**Keywords:** *Hemicellulose, polyhydroxybutyrate, poly (lactic acid), blends, solvent casting, thermal properties.*

## 1. Introduction

Production of biopolymers from lignocellulosic materials has recently gained momentum. Among the main components of lignocellulosic materials, hemicellulose comprises between 20% to 35% of the total composition and has good water solubility and biodegradability[1-3]. Previous literature has shown the advantages of using hemicellulose in different material applications[4-7]. For example, hemicellulose is considered a potential alternative in food packaging[4] and biomedical[5] applications. In addition, hemicellulose has been applied as an adsorbent for water treatment[6] and biofuel products[7]. Nevertheless, hemicelluloses present intrinsic drawbacks such as poor mechanical properties, low solubility in different solvents, and hydrophilic and amorphous structures[4]. One alternative for surpassing mechanical and thermal properties issues could be blending hemicellulose with other polymers.

The investigation of blends from aliphatic polyesters, such as poly (3-hydroxybutyrate) (PHB) or poly (lactic acid) (PLA), is known as a possibility to improve the properties and applications of polysaccharides[8]. Moreover, PHB and PLA have a high capacity to improve their thermal properties and solubility when used in composites and blends[9]. Regarding literature on PLA, this polymer has not yet been extensively used in applications due to its specific characteristics and properties, such as its high cost, fragility, low ductility, and low glass transition temperature ($T_g$)[10,11]. In addition, the studies on blending PHB and PLA are more common with cellulose[12,13] and starch[8,14] than with hemicelluloses, with limited investigations on the literature (Table 1).

The solvent casting technique appears as a solution for solubility, allowing the mixture of the polymers in a dissolved state that are widely used to obtain biodegradable polymer films[17]. Furthermore, polar and non-polar solvents can affect the miscibility between hydrophilic and hydrophobic polymers, thus promoting a better merging between polymers and hemicelluloses. Acetic acid (non-polar) and chloroform (polar) were previously investigated as solvents for PHB and PLA polymers[18,19]. The studies reported chloroform as a suitable solvent for PHB and PLA. However, chloroform is detrimental to human health and the environment. Hence, acetic acid might be an alternative in blends with polyesters, leading to the best intermolecular interaction between the ester and carboxyl groups of the acid with the polymer structure[20].

Plasticizer agents such as glycerol (a biodegradable, non-toxic, low-cost natural compound) have also been addressed in the literature to improve miscibility between

*e-mail: michaella.socorro@gmail.com

**Table 1.** Summary of studies on blends of PHB and PLA with polysaccharides describing the applied solvent, analytical techniques and evaluation/optimization method.

| Material | Solvent | Analysis | Evaluation | Ref. |
|---|---|---|---|---|
| PHB<br>Chitosan | Hexafluoroisopropanol | SEM<br>Water contact angle<br>X-ray; FTIR<br>DSC<br>Mechanical | Statistical analysis by conventional methods | [15] |
| PHB<br>Cellulose | Chloroform | SEM<br>X-ray<br>Water absorption<br>Water vapor permeability<br>Mechanical | - | [13] |
| PHB<br>Starch | Chloroform | TG<br>Mechanical | - | [8] |
| PLA<br>Starch | Chloroform | TG<br>Mechanical<br>Charpy<br>FTIR<br>SEM | - | [16] |
| PLA<br>Thermoplastic starch | Ethyl acetate | SEM<br>X-ray; FTIR<br>TG<br>Mechanical | Analysis of variance (ANOVA) | [14] |
| Hemicellulose<br>PHB<br>PLA | Acetic acid<br>Chloroform | TG<br>SEM<br>FTIR | MCDA | Present study |

polyesters[21]. Glycerol can also incorporate into hemicellulose films, reducing their fragility and improving flexibility[22].

This work therefore aims to investigate how acetic acid (non-polar) and chloroform (polar) affect the thermal properties of blends composed of hemicellulose and PHB (Hemi/PHB) and hemicellulose and PLA (Hemi/PLA). To our understanding (Table 1), no study has yet assessed the blend of hemicellulose, PLA, and PHB in different proportions (10-50%) by cross-evaluating thermal properties and morphological aspects and applying a multicriteria decision analysis (MCDA) approach to identify optimum blend. Therefore, the novelty of this study relies on i) assessing different solvents for bio-based blend production via solvent casting; ii) performing different analytical techniques (Fourier transform infrared spectroscopy, thermogravimetric analysis, and scanning electron microscopy) to characterize the produced blends; and iii) applying an MCDA method to the obtained thermal properties to identify witch solvent (acetic acid and chloroform), hemicelluloses proportion (10–50%), and bio-based polymer (PHB and PLA) are suitable for producing biodegradable blends. The results provide new insights into bio-based blends and their properties.

## 2. Materials and Methods

### *2.1. Materials*

The hemicellulose was extracted from jute fibers (*Corchorus capsularis*) provided by Sisalsul Industry and Commerce LTDA. The chemical reagents were supplied from Greentec: glacial acetic acid (99.7%), chloroform (99%), ethanol (99.5%), and potassium hydroxide (85% purity). Glycerin (99.5%) was purchased from Cromoline. The biopolymers were polyhydroxybutyrate pellets (PHB, *Mw*: 190 kDa, BRS Bulk Bio-Pellets, Bulk Reef Supply, Golden Valley, MN, EUA) and poly (lactic acid) pellets (PLA, *Mw*: 390 kDa, 4043 D sediments, NatureWorks LCC, Minnetonka, MN, EUA).

### *2.2. Obtaining the hemicellulose from jute fibers*

The hemicellulose extraction methodology was developed in a previous work[23] using a light alkaline treatment. About 10 g of raw jute fibers were soaked in 200 mL of distilled water at 25 °C for 1 h to remove impurities from the fibers and facilitate the hemicellulose extraction. The fibers were then added to 200 mL of a KOH 10% (w/v) solution under mechanical stirring at 50 rpm and orbital shaking at 250 rpm for 3 h at 25 °C. After 24 h, the solution was centrifuged at 4000 rpm for 5 min. A 250 mL glacial acetic acid and ethanol 1:10 (v/v) solution was added to the liquor to precipitate the hemicellulose. Subsequently, the resulting solution was filtered and the hemicellulose portion was washed with distilled water (200 mL) three times and dried at room temperature for 24 h. The liquor was filtrated and the pH was adjusted to 4.8 using acetic acid.

### *2.3. Production of hemicellulose film*

Hemicellulose is not soluble in acetic acid or chloroform. Before being mixed with the biopolymers, hemicellulose was

dissolved in distilled water at 70 °C for 10 min under constant stirring to a concentration of 0.05 g/mL and centrifuged at 4000 rpm for 10 min. After that, it was poured into a glass plate (26 mm x 76 mm) to obtain the films.

### 2.4. Production of the blends with acetic acid and chloroform

An overview of the hemicellulose concentration in new materials is essential since biopolymers can be compatible with a specific application within a particular composition (properties) range. Therefore, PHB or PLA blends were prepared using the solvent casting method to investigate the hemicellulose concentration in the blends for five different compositions (10, 20, 30, 40, and 50 wt%)[8,15]. The blends were prepared using acetic acid (AA) and chloroform (CHL) as a solvent and followed the method developed by[18]. In addition, PHB/hemicellulose blends using AA as the solvent were tested with glycerol as a plasticizer to improve the compatibility/homogeneity of these blends. The blend codes considering the different concentrations (wt%) of hemicellulose, PHB, PLA, glycerol presence, and solvent type (AA or CHL) are shown in Table 2.

First, the PHB or PLA blends with hemicellulose using AA and glycerol were produced. The concentration of the casting solution was 0.05 g/mL, and the pellets of PHB or PLA were individually mixed with AA using a magnetic stirrer for approximately 50 min at the boiling temperature of AA (~118 °C) and the melting temperature of PHB (~170 °C) or PLA (~150 °C). Next, the hemicellulose solution was immersed in the PHB/AA or PLA/AA solution to produce the blends, followed by magnetic stirring at 80 °C for 40 min. Finally, the glycerol, acting as a plasticizer, was added to the mixture of hemicellulose and PHB blends cast with AA.

Second, the PHB or PLA blends with hemicellulose using CHL were produced. The hemicellulose solution (0.05 g/mL) was poured into the PHB/CHL or PLA/CHL solution (0.05 g/mL) under magnetic stirring at 70 °C. Next, PHB or PLA was dissolved in CHL near their boiling point (~70 °C) under magnetic stirring for 30 min.

Finally, the blend solution was deposited on glass plates (26 mm x 76 mm) for both solvents and the films were formed after the complete evaporation of the solvents at room temperature.

### 2.5. Thermogravimetry (TG) and differential scanning calorimetry (DSC) characterization

TG and DSC were conducted using an SDT Q600 TA Instruments thermal analyzer ($10^{-4}$ g precision). TG equipment was adequately calibrated[24] and experimental error between experiments was controlled below 0.5%[25]. Polymer samples of 10 mg were placed in alumina pans under an $N_2$ atmosphere at a flow rate of 50 mL/min from 25 °C to 600 °C at a 10 °C/min heating rate. The crystallinity degree ($X_c$) of the blends was calculated using Equation 1 and DSC data.

$$\%X_c = \Delta H_m \,.100 / \Delta H_{m100\%} \,.w \quad (1)$$

where $\Delta H_m$ is the melting heat associated with the pure crystalline material (146 J/g for PHB and 96 J/g for PLA) and $w$ is the weight fraction of the PHB or PLA in the blend. The glass transition temperature ($T_g$) and the melting temperature ($T_m$) were determined using the "TA Universal Analysis" software, considering the first baseline and thermal event (second endothermic event without mass change), respectively.

### 2.6. Fourier transform infrared spectroscopy (FTIR)

The pure polymers and blends were ground and mixed with dry KBr to prepare 120 mg tablets (1.5 wt% of sample in KBr). The samples were analyzed using the transmission

**Table 2.** Blend codes based on hemicellulose, PHB, PLA content (wt%), glycerol (wt%) presence, and solvent type (AA or CHL).

| Blend Codes | | Hemicellulose | Glycerol | Solvent |
|---|---|---|---|---|
| PHB | PLA | (wt%) | (wt%) | |
| Hemi-AA | PLA-AA | 100 | - | AA |
| PHB-AA | Hemi10/PLA-AA | - | - | AA |
| Hemi10/PHB-AA | Hemi20/PLA-AA | 10 | - | AA |
| Hemi20/PHB-AA | Hemi30/PLA-AA | 20 | - | AA |
| Hemi30/PHB-AA | Hemi40/PLA-AA | 30 | - | AA |
| Hemi40/PHB-AA | Hemi50/PLA-AA | 40 | - | AA |
| Hemi50/PHB-AA | | 50 | - | AA |
| Hemi10/PHBG-AA | | 10 | 25 | AA |
| Hemi20/PHBG-AA | | 20 | 20 | AA |
| Hemi30/PHBG-AA | | 30 | 15 | AA |
| Hemi40/PHBG-AA | | 40 | 10 | AA |
| Hemi50/PHBG-AA | | 50 | 5 | AA |
| Hemi-CHL | PLA-CHL | 100 | - | CHL |
| PHB-CHL | Hemi10/PLA-CHL | - | - | CHL |
| Hemi10/PHB-CHL | Hemi20/PLA-CHL | 10 | - | CHL |
| Hemi20/PHB-CHL | Hemi30/PLA-CHL | 20 | - | CHL |
| Hemi30/PHB-CHL | Hemi40/PLA-CHL | 30 | - | CHL |
| Hemi40/PHB-CHL | Hemi50/PLA-CHL | 40 | - | CHL |
| Hemi50/PHB-CHL | | 50 | - | CHL |

Hemi - Hemicellulose; AA - acetic acid; CHL - chloroform; PHB - polyhydroxybutyrate; PLA - poly (lactic) acid; PHBG - PHB with glycerol.

method and a NICOLET IS10 spectrometer (Thermo Scientific) from 4000 to 400 $cm^{-1}$ with 64 scans was collected at 4 $cm^{-1}$ intervals.

### *2.7. Scanning electron microscopy (SEM)*

The materials were metalized with gold and analyzed using a scanning electron microscope (JEOL JSM-7001F). The images were captured using a voltage of 15 kV and 200X and 1000X magnification.

### *2.8. Multicriteria decision analysis*

Usually, the choice of a better product depends on achieving the most satisfactory characteristics, considering several criteria that account for several targets. Understanding that there is no global solution for all products concurrently and multiple solutions can be achieved for different purposes, a decision analysis must be applied to select the ideal process variables[26]. Previous studies[26-29] modeled and applied a multicriteria decision analysis (MCDA) to evaluate a multicriteria problem involved in biomass valorization routes.

In this study, the MCDA was modeled and discussed to assess the compatibility between polymers and to verify which has the best polymer-solvent interaction through the thermal characterization results considering casting solvent, polymer, and hemicelluloses proportion.

The multicriteria decision problem relied on assessing which process conditions are best to produce higher-quality biodegradable polymer blends based on the melting temperature of the blends $T_m$ (°C), melting heat associated with the pure crystalline material $\Delta H_m$ (J/g), and the crystallinity degree $\%X_c$ indicators. The indicators were chosen considering the maintenance of thermal stability after the blend preparation, the necessary energy needed to dissolve the crystal parts in PLA and PHB, the further maintenance of the crystallinity degree, and the available experimental techniques.

The decision analysis was set as a minimization problem. Therefore, the best to be higher criteria were dealt with as the numeric inverse (1/higher = lower). In the present work, the decision problems were structured based on the dominance analysis (weak dominance (WD) and strong dominance (SD) and a metric distance ($d_n$) based on compromise programming[30]. Modeling formulation and the MCDA code can be found in previous works[26,27].

## 3. Results and Discussion

### *3.1. Visual appearance of the pure polymers and blends*

The visual appearance of the pure polymers and their films cast with AA and CHL can be observed in Figure 1. The aspect of the films of PHB and PLA solubilized with CHL exhibited a more homogeneous surface than AA, which is the common solvent used for these polymers[18].

PHB and PLA can interact entirely with non-polar (AA) solvents because they present an amphiphilic structure composed of hydrophilic and hydrophobic parts[31]. However,

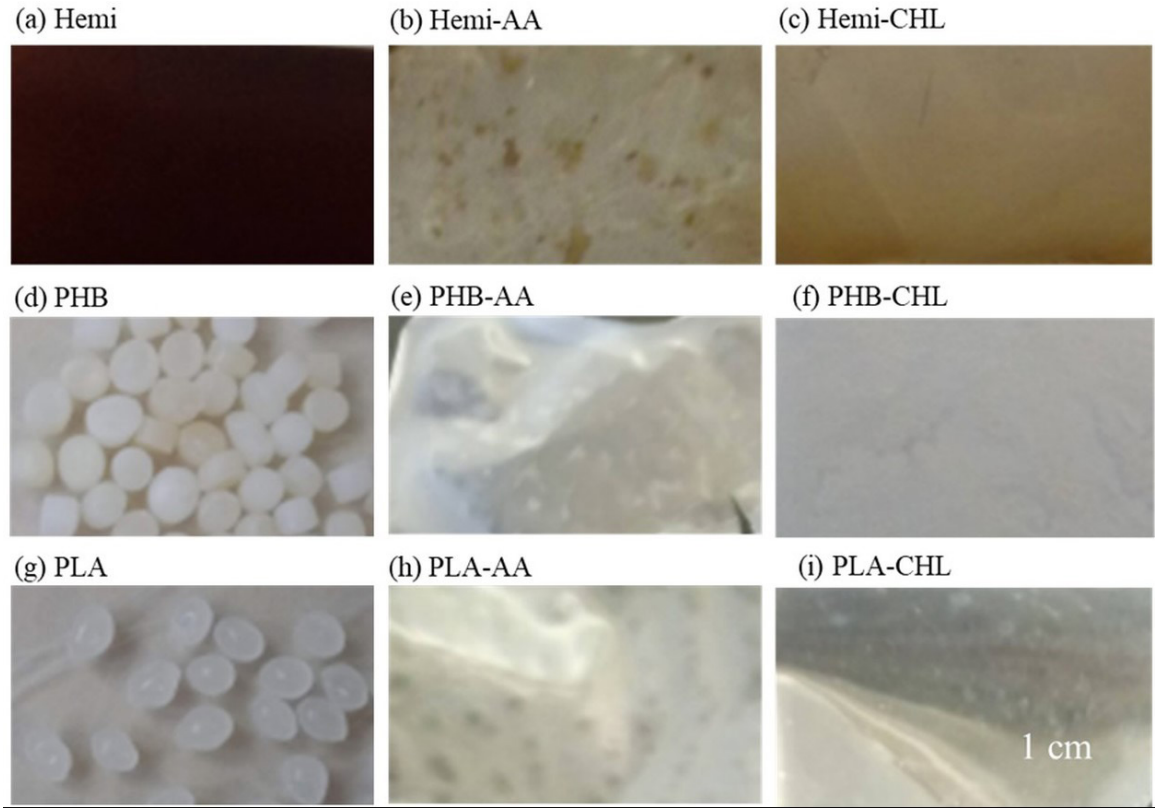


**Figure 1.** Images of hemicellulose (Hemi), PHB, and PLA films after solvent casting with acetic acid (AA) or chloroform (CHL).

each polymer has a specific incompatibility with AA[11], which allows its dissolution up to a particular limit and causes irregular areas of the film, as observed by[18].

The hemicellulose extracted from curaua fiber has a low molecular weight of around 118,000 g/mol[32] (probably similar to hemicellulose from jute fiber due to the same extraction method) and has a typical degree of polymerization (DP) of 140[33]. The literature reports the high complexity film formation from low molecular weight polymers[34]. Nevertheless, Figure 1 shows that the obtained films from hemicellulose showed good flexible film formation.

The Hemi-AA showed agglomerated areas throughout the film. This observation can be associated with poor polymer-solvent interaction. On the other hand, Hemi-CHL showed lighter regions on the film surface, indicating that the hemicellulose could be partially soluble in CHL by dissolving its side chains[31].

The blends of hemicellulose with PHB and PLA prepared by solvent casting using the different solvents showed relevant differences in the visual aspect of the samples. Figure 2 shows the PHB blends cast with various solvents, hemicellulose content, and glycerol used as a plasticizer.

The Hemi/PHB-AA blends resulted in damaged and brittle films (Figure 2), making it impossible to form continuous films. Nevertheless, all these samples exhibited homogeneity in their mixture at all concentrations, indicating good compatibility between the solvent and the polymers.

In contrast, the Hemi/PHB-CHL blends reported immiscibility between hemicellulose and CHL, leading to polymer separation and scattering of hemicellulose in most compositions (Figure 2). The Hemi50/PHB-CHL sample also presented the most homogeneous film and excellent dispersion of hemicellulose compared to the other compositions. This behavior may occur due to a higher concentration of hemicellulose and, consequently, less CHL content to obtain the blend.

When plasticized with glycerol, the samples with Hemi10/PHBG-AA and Hemi20/PHBG-AA showed good miscibility. However, it was impossible to obtain continuous films, as Quispe et al.[35] observed. Their results on PHB with 20 and 30 wt% glycerol resulted in materials that were sticky and difficult to handle[35].

Figure 3 shows the Hemi/PLA blends cast with different solvents and hemicellulose content. The blends with 10–30 wt% of hemicellulose formed a powder but the blends with 40–50 wt% of hemicellulose resulted in foam and film phases. A similar behavior was reported by the previous study[36], where the foam form and separated phases were observed when using hemicellulose extracted from wood at 10 and 20 wt%.

The visual aspect of Hemi/PLA-CHL blends showed these polymers' immiscibility. The hemicellulose was dispersed on the film's surface due to differences in solubility and polarity[36].

### *3.2. Chemical characterization of the blends by FTIR*

Figure 4 shows the FTIR spectra of the hemicellulose/PHB and hemicellulose/PLA blends. All spectra from the samples with hemicellulose and PHB showed a peak around 3400 $cm^{-1}$, corresponding to hydroxyl groups present in hemicellulose, residual solvents, and increased O–H groups[37]. The differences observed around 1257 $cm^{-1}$ and 1036 $cm^{-1}$ in Hemi/PHB blends (Figure 4c) can be attributed to intermolecular bonds and the crystallinity, which was decreased by blending with glycerol[35]. The bands around 2900–2750 $cm^{-1}$ are due to overlapping C-H deformations

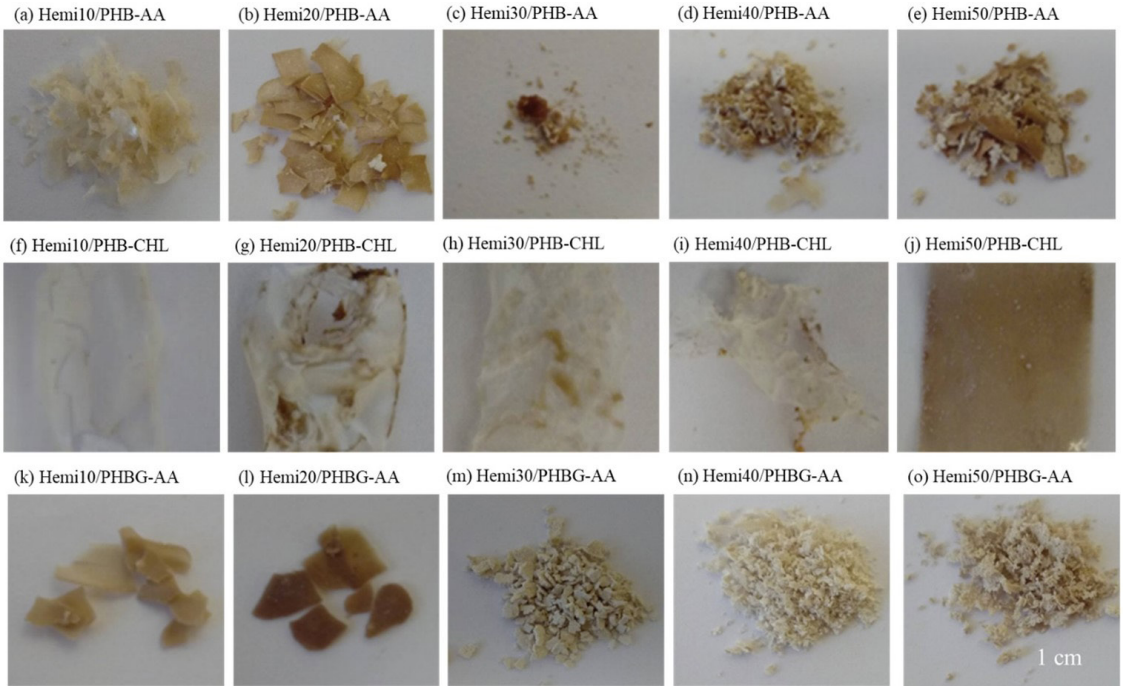


**Figure 2.** Blends of PHB cast with different solvents (AA or CHL), hemicellulose content (Hemi), and the addition of glycerol (G).

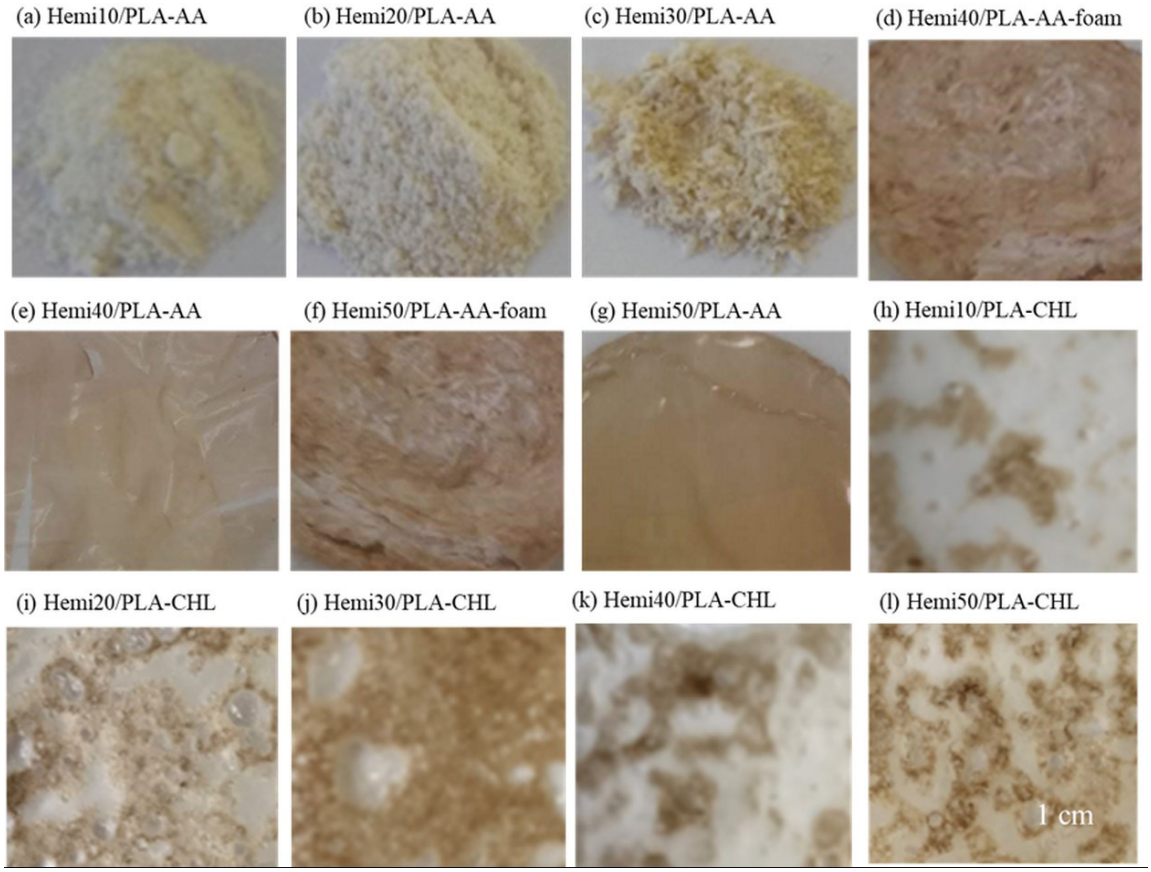


**Figure 3.** PLA blends cast with different solvents (AA or CHL) and hemicellulose content (Hemi). Two phases were evidenced for Hemi40/PLA and Hemi50/PLA, foam and film.

of PHB and PLA and the vibrations of the methyl and methylene groups of the hemicellulose[12,38].

The bands between 2989 $cm^{-1}$ and 2870 $cm^{-1}$ in the spectrum of Hemi/PLA-CHL (Figure 4e and f) indicate the presence of symmetrical and asymmetrical elongations of the methyl and methylene groups of the hemicellulose[37] and PLA. Hemi10/PLA-AA, Hemi20-PLA-AA, and Hemi30/PLA-AA exhibited higher intensities around 1755 $cm^{-1}$. The Hemi40/PLA-AA, Hemi40/PLA-AA-foam, and Hemi50/PLA-AA-foam blends presented bands referring to the PLA-AA, but their low intensity indicated a lack of interaction[36]. This may also be related to the hemicellulose changes in the crystalline region of the polymers, as observed in blends with chitosan[15].

The Hemi40/PLA-AA and Hemi50/PLA-AA presented the band around 1550 $cm^{-1}$ associated with the esters and acetyl groups of the hemicellulose[19]. The band around 1355 $cm^{-1}$ appeared in all blends, which might be related to the bending or asymmetrical deformation of CH from the $CH_3$ group of the PLA[38] or the symmetrical deformation of $CH_2$ and C-OH of the hemicellulose[39].

Comparing the spectral bands (Figure 4a and b) from 1720 $cm^{-1}$ to 1530 $cm^{-1}$ for both solvents, it is noted that AA showed better intermolecular interactions than CHL. Meanwhile, the band around 1500 $cm^{-1}$ (Figure 4b) refers to the hemicellulose, which indicates incompatibility between hemicellulose and CHL. This solvent reacted with the non-polar part of PHB and the side chains of hemicellulose. The decrease in the intensity of the carbonyl band around 1750 $cm^{-1}$ in some blends can relate to the lack of association of some compounds in the solution, that is, a low interaction of hemicellulose with CHL.

The blends showed better interaction with AA as a solvent. Although the PHB and PLA had better interaction with CHL, this solvent disperses the hemicellulose groups and causes the separation of the film surface, as seen in Figure 2 and 3.

### *3.3. Thermogravimetry (TGA) and differential scanning calorimetry (DSC)*

The TGA, its derivative thermogravimetric (DTG) and DSC curves for Hemi/PHB blends are shown in Figure 5. After removing the moisture (~105 ºC), the pure hemicellulose (H100) degradation occurs between 200–300 ºC, which is in line with[40,41]. The blend degradation for both solvents and plasticizer (glycerol) occurred at temperatures below the pure PHB (~270–290 °C). The temperature degradation decreases for the PHB blends, showing the chemical influence of the hemicellulose groups (Figure 5a).

The results for Hemi/PHB-AA showed two degradation peaks, except for Hemi10/PHB-AA, which presented the same behavior as PHB-AA. However, its degradation temperature was reduced, remaining at around 224 °C. As seen from the

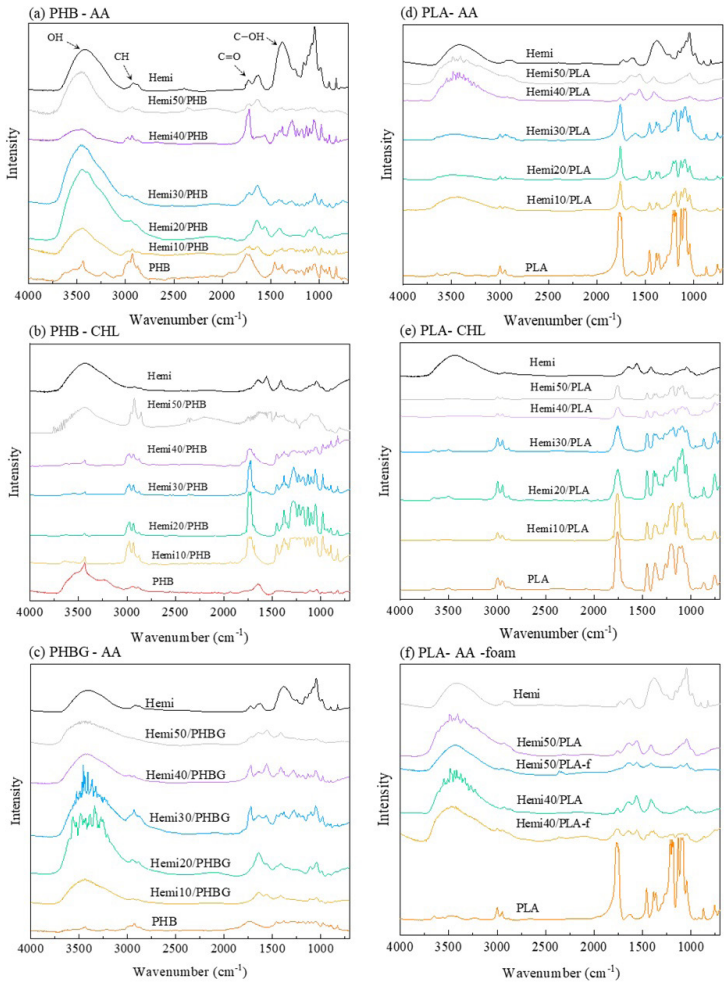


**Figure 4.** FTIR spectra of Hemi/PHB (a) Acetic acid (AA), (b) Chloroform (CHL), and (c) Chloroform and glycerol; and Hemi/PLA (d) Acetic acid, (e) Chloroform (CHL), and (f) Acetic Acid (AA).

DTG curve (Figure 5b), the Hemi/PHB-CHL blends exhibited two degradation stages: the first peak between 180–240 °C and the second between 266–280 °C. The hemicellulose influenced the decrease in thermal stability[36], which is in line with the influence of starch on the thermal behavior of PLA/starch[14] and PHB/starch[8] blends. Furthermore, the lower thermal stability might be associated with the residual solvents, which might affect thermal behavior[17].

The Hemi/PHB-AA blends with the plasticizer glycerol showed a degradation stage between 207–217 °C (Figure 5g). The temperature and intensity of the peaks in the blends decreased for pure hemicellulose and PHB. This behavior might be attributed to a change in the hemicellulose structure, in addition to removing part of the structure PHB present in the blend[42].

The DSC curves for the blends of Hemi/PHB cast with the solvents AA (Figure 5c), CHL (Figure 5f), and AA and glycerol (Figure 5i) showed a different performance than pure polymers. The Hemi/PHB blends cast with both solvents presented two stages of degradation; the first is related to the melting point ($T_m$) and the second is associated with the degradation temperature of the samples.

The melting temperature of the blends ($T_m$) prepared with AA presented the most intense peak. However, PHB-CHL exhibits a lower $T_m$ than PHB-AA. Similar behavior was observed in PHB/starch blends using hexafluoroisopropanol (polar) as the solvent, with a decrease in $T_m$ as the starch concentration increases[15]. PHB/hemicellulose blends with glycerol showed a reduction in the melting temperature due to the mobility of the plasticizer in the polymer structure. It is also observed that the melting enthalpy ($\Delta H_m$) of all blends decreased in intensity as well as the percentage of crystallinity ($X_c$), indicating that less energy was needed to melt the blends, which is in line with[35]. Both parameters are further discussed in the MCDA (Section 3.4).

The TGA, DTG, and DSC curves of Hemi/PLA-AA are shown in Figure 6. Figure 5 despite the PLA-AA blends showing a lower degradation temperature than pure PLA (~345–360 °C) and a higher degradation temperature than Hemi/PHB-AA. The blends of Hemi40/PLA-AA and Hemi50/PLA-AA that presented foam form (Figure 6d and e) reported

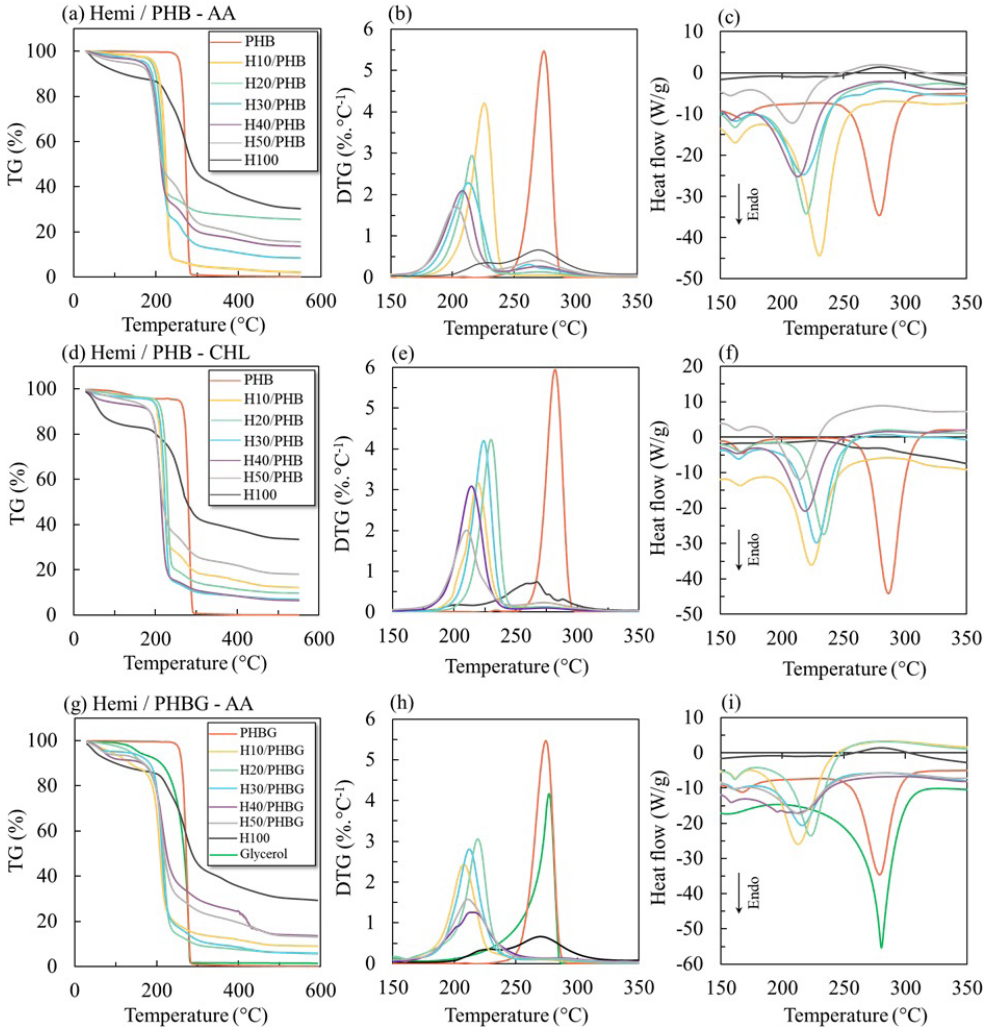


**Figure 5.** The TGA, DTG, and DSC curves for Hemi/PHB blends cast with (a, b, and c) acetic acid (AA), (d, e, and f) chloroform (CHL), and (g, h, and i) with the glycerol addition (G) as a plasticizer and acetic acid (AA) as the solvent.

a similar decomposition temperature to Hemi-AA probably because of hemicellulose concentration, which caused the separation of PLA in the blend. The results corroborate the previous study on PLA blends and microcrystalline cellulose (MCC) as reinforcement, which reported that the distribution of MCC increases the agglomeration and thus decreases the thermal stability[12].

Regarding the glass transition temperature ($T_g$), PLA-AA presented a reduction in $T_g$ to approximately 35 °C. The blends Hemi10/PLA-AA, Hemi40/PLA-AA, and Hemi50/PLA-AA presented $T_g$ values of 62, 53, and 55 °C, respectively. This reduction in $T_g$ might be associated with the hydroxyl groups of hemicellulose. According to what was reported for PLA/starch blends, the moisture content of starch acted as a plasticizer, reducing the $T_g$[16]. We also observed that the Hemi20/PLA-AA and Hemi30/PLA-AA showed two degradation temperatures: the first exothermic peak between 257–262 °C (hemicellulose degradation[23]) and the second endothermic peak between 280 °C and 295 °C (PLA degradation). The results align with PLA/galactoglucomannan blends, which reported the same temperature degradation[36]. The blends with the foam form presented the lowest crystallinity values, which corroborates with the FTIR results that showed functional groups in hemicellulose.

### *3.4. Multicriteria decision analysis*

The MCDA was performed considering two distinct decision analyses. Table 3 shows the thermal properties of PHB and PLA with AA as the solvent. Meanwhile, Table 4 displays the blend results for PHB with the AA and CHL solvent. The last four columns represent the results in % for metric distance ($d_n$), weak dominance (WD), strong dominance (SD), and the total success rate (TSR) in %[30]. For the multicriteria results, green was chosen to represent the best results and red indicates the worst results.

The MCDA contemplated as criteria the melting temperature of the blends $T_m$ (°C), melting heat associated with the pure crystalline material $\Delta H_m$ (J/g), and the crystallinity degree $\%X_c$ indicators. The melting temperature was previously

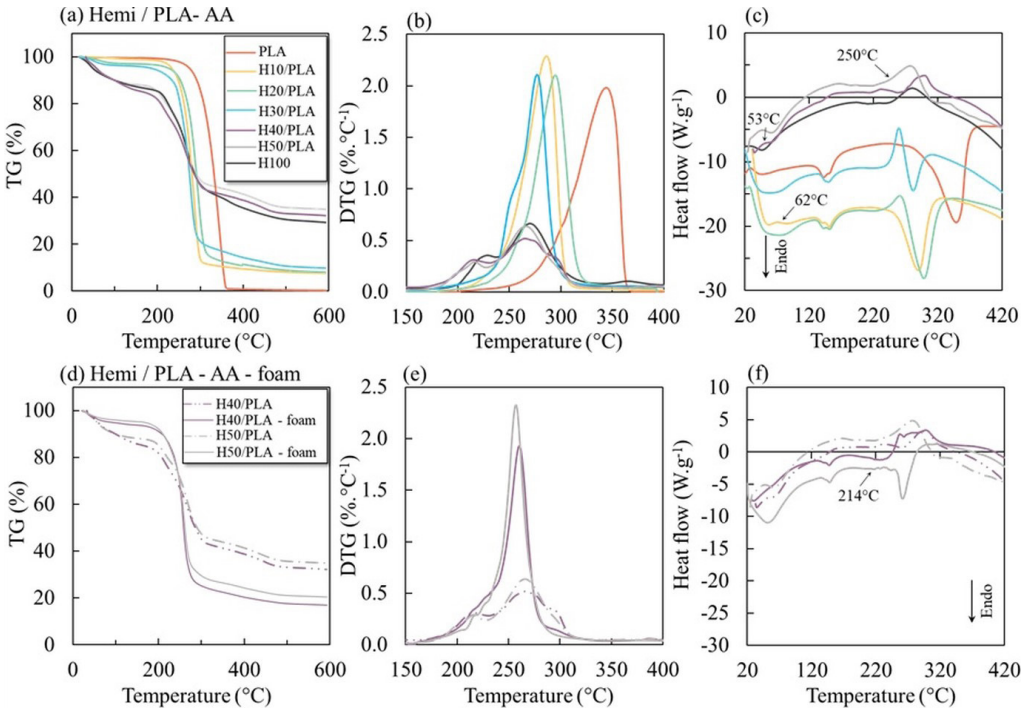


**Figure 6.** TGA, DTG, and DSC curves for Hemi/PLA blends cast with (a, b, and c) acetic acid (AA), (d, e, and f) Hemi40/PLA foam and film.

**Table 3.** Multicriteria analysis for PHB and PLA with AA as the solvent.

| Polymers and Blends | $T_m$ | $\Delta H_m$ | $X_c$ | $d_n$ | WD | SD | $d_n$ | WD | SD | TSR |
|---|---|---|---|---|---|---|---|---|---|---|
| PHB-AA | 167.83 | 32.42 | 22.21 | 0.1474 | 10 | 16 | 86% | 59% | 94% | 80% |
| Hemi10/PHB-AA | 162 | 33.29 | 25.33 | 0.1100 | 9 | 16 | 89% | 53% | 94% | 79% |
| Hemi20/PHB-AA | 161.71 | 18.42 | 15.77 | 0.2998 | 4 | 14 | 71% | 24% | 82% | 59% |
| Hemi30/PHB-AA | 161.85 | 15.78 | 15.44 | 0.3343 | 4 | 14 | 68% | 24% | 82% | 58% |
| Hemi40/PHB-AA | 159 | 14.9 | 17.01 | 0.3230 | 2 | 13 | 69% | 12% | 76% | 52% |
| Hemi50/PHB-AA | 158.1 | 10.95 | 15 | 0.4691 | 0 | 10 | 55% | 0% | 59% | 38% |
| Hemi10/PHBG-AA | 162.08 | 6.55 | 6.9 | 1.0449 | 0 | 15 | 0% | 0% | 88% | 29% |
| Hemi20/PHBG-AA | 161.28 | 25.5 | 29.11 | 0.1040 | 8 | 16 | 90% | 47% | 94% | 77% |
| Hemi30/PHBG-AA | 161.62 | 10.47 | 13.04 | 0.5211 | 2 | 12 | 50% | 12% | 71% | 44% |
| Hemi40/PHBG-AA | 158.35 | 6.47 | 8.86 | 0.9338 | 0 | 8 | 11% | 0% | 47% | 19% |
| Hemi50/PHBG-AA | 159.13 | 8.44 | 12.85 | 0.6459 | 1 | 10 | 38% | 6% | 59% | 34% |
| PLA-AA | 143.16 | 39.15 | 42.1 | 0.1470 | 0 | 16 | 86% | 0% | 94% | 60% |
| Hemi10/PLA-AA | 151.25 | 23.14 | 27.65 | 0.1433 | 3 | 15 | 86% | 18% | 88% | 64% |
| Hemi20/PLA-AA | 152.28 | 22.78 | 30.62 | 0.1369 | 3 | 16 | 87% | 18% | 94% | 66% |
| Hemi30/PLA-AA | 150.24 | 17.34 | 26.64 | 0.2213 | 2 | 13 | 79% | 12% | 76% | 56% |
| Hemi40/PLA-AA-f [a] | 147.62 | 10.51 | 18.84 | 0.4660 | 0 | 10 | 55% | 0% | 59% | 38% |
| Hemi50/PLA/AA-f a | 148.39 | 9.05 | 19.46 | 0.5587 | 0 | 10 | 47% | 0% | 59% | 35% |

[a] foam, $T_m$ in ºC, $\Delta H_m$ in J.g$^{-1}$, and $X_c$ in %.

discussed in Section 2.3. Next, the $\%X_c$ (which is a function of the $\Delta H_m$) is discussed.

Table 3 shows that Hemi10/PHB-AA had the highest crystallinity (considering PHB blends with AA as the solvent without glycerol), with 25.33% compared to 22.21% for pure PHB-AA. The blend crystallinity was reduced for the higher hemicellulose concentrations (>20 wt%), except for Hemi20/PHBG-AA. This behavior might be associated with the mass decrease of PHB (within the blend). Moreover, crystallinity might be linked to the interaction between the hydroxyl groups (from glycerol) with the ester bonds (from PHB and hemicellulose)[42]. This decrease in the blend's crystallinity can also be associated with a weight loss of glycerol at around 155 °C.

As expected, Hemi/PLA-AA blends presented lower crystallinity than PLA-AA (42.1%) and for 10, 20, and 30wt% hemicellulose concentration, the crystallinity showed a minor difference of around 30%. The blends of the Hemi40/PLA-AA-foam and Hemi50/PLA-AA-foam showed a crystallinity between 18.8% and 19.5%.

**Table 4.** Multicriteria analysis for PHB with AA and CHL as the solvent.

| Blends | $T_m$ | $\Delta H_m$ | $X_c$ | $d_n$ | WD | SD | $d_n$ | WD | SD | TSR |
|---|---|---|---|---|---|---|---|---|---|---|
| PHB-AA | 167.83 | 32.42 | 22.21 | 0.0511 | 9 | 11 | 94% | 75% | 92% | 87% |
| Hemi10/PHB -AA | 162.00 | 33.29 | 25.33 | 0.0372 | 4 | 11 | 96% | 33% | 92% | 74% |
| Hemi20/PHB -AA | 161.71 | 18.42 | 15.77 | 0.2488 | 1 | 7 | 72% | 8% | 58% | 46% |
| Hemi30/PHB-AA | 161.85 | 15.78 | 15.44 | 0.2910 | 1 | 6 | 68% | 8% | 50% | 42% |
| Hemi40/PHB-AA | 159.00 | 14.90 | 17.01 | 0.2810 | 1 | 7 | 69% | 8% | 58% | 45% |
| Hemi50/PHB-AA | 158.10 | 10.95 | 15.00 | 0.4481 | 0 | 2 | 50% | 0% | 17% | 22% |
| PHB-CHL | 168.43 | 23.78 | 16.29 | 0.2065 | 6 | 11 | 77% | 50% | 92% | 73% |
| Hemi10/PHB-CHL | 166.47 | 12.12 | 9.22 | 0.6722 | 0 | 8 | 26% | 0% | 67% | 31% |
| Hemi20/PHB-CHL | 166.60 | 20.39 | 17.46 | 0.1878 | 7 | 10 | 79% | 58% | 83% | 74% |
| Hemi30/PHB-CHL | 165.15 | 18.15 | 17.76 | 0.2064 | 5 | 10 | 77% | 42% | 83% | 67% |
| Hemi40/PHB-CHL | 164.17 | 13.77 | 15.72 | 0.3297 | 2 | 7 | 64% | 17% | 58% | 46% |
| Hemi50/PHB-CHL | 163.71 | 6.85 | 9.38 | 0.9037 | 0 | 6 | 0% | 0% | 50% | 17% |

$T_m$ in ºC, $\Delta H_m$ in J.g$^{-1}$, and $X_c$ in %

The Hemi/PHB blends showed that the total percentage decreases with the hemicellulose content from all the blends concerning the solvent used, differently from Hemi/PHBG blends, which do not present a defined tendency with hemicellulose concentration. The presence of glycerol might cause higher mobility, affecting the PHB crystallinity. In the case of the Hemi/PLA blends, the total percentage was similar to that of PLA-AA.

The multicriteria analysis for PHB and PLA with AA as the solvent (Table 3) showed a TSR of 80% for PHB. Meanwhile, PLA presented lower TSR with around 60%. Hemi10/PHB-AA showed the highest TSR of 79%. Meanwhile, when combined with the glycerol plasticizer (Hemi10/PHBG-AA), it decreased to 29%. However, for the Hemi20/PHBG-AA, a TSR of 77% due to the higher percentage of $X_c$. Regarding PLA-AA blends, an increasing tendency for 10 and 20 wt% of hemicellulose was revealed. Adding more hemicelluloses to the blend showed a decrease in TSR for 30–50 wt% (where 40 and 50 wt% had foam form). We can therefore infer that the hemicellulose directly affects the $X_c$ in the blends, as well as their miscibility.

When analyzing PHB-AA (Table 4), a maximum TSR of 87% was reported, while PHB-CHL obtained a TSR of 73%. For the lower hemicellulose concentrations, the Hemi10/PHB-AA blend showed a TSR of 74%, while for Hemi10/PHB-CHL, it decreased significantly to 31%. In the same way, for higher hemicellulose concentrations, the success rate drastically decreases, as the mixture of Hemi50/PHB-AA presented 22% and for Hemi50/PHB-CHL only 17% success rate.

These results also corroborate the visual appearance of the mixtures, where the blends molded with CHL as a solvent presented the lowest TSR, as observed in the phase separation of the polymers in Figures 2, 3. In contrast, the blends molded with AA as the solvent obtained the best TSR, corroborating the visual appearance that was more homogeneous (than the blends molded with CHL).

### *3.5. Morphology*

Figure 7 shows the SEM images of the blends that formed films or presented homogeneous regions. Hemi20/PHB-AA presented dispersion areas along with the surface film. This dispersion can be associated with hemicellulose, which is not entirely soluble in AA. Lopera et al.[43] described that the PHB and PLA blends with cellulose nanocrystals could agglomerate along with the blend. This event is characteristic of the polysaccharide used. In the Hemi/PLA-AA blend, particles are dispersed in the blend. The same behavior was observed with Hemi/PHB-AA. These particles may refer to the PLA crystals or residues from the hemicellulose extraction and blend manufacturing. Some particles (indicated by circles) may occur due to differences in the solubility of the two polymers and cracks on the film surface. Shao et al.[1] reported that the roughness of the films increases with the presence of carboxylic acids due to the greater intermolecular interactions by hydrogen bonding. Therefore, the carboxyl groups in the acid react with the hydroxyl groups in hemicellulose and PLA. Carboxylic acids in the blend structure can lead to a rough appearance of pores[44]. More ordered regions (indicated by the arrows) can be observed in the Hemi10/PHBG-AA and Hemi20/PHBG-AA blends due to the presence of the plasticizer film[35].

In addition, separate regions are noted in the blend (indicated by circles). These distinct regions may occur due to the difference in the solubility of the polymers with the solvent used. Some gaps associated with the inefficient mixing between the polymers and the miscibility of the materials were observed[43]. The micrographs of the Hemi/PHB-CHL blends presented a smooth appearance with few dispersed particles associated with hemicellulose, which is not soluble in CHL. The Hemi50/PHB-CHL with the highest concentration of hemicellulose showed large particles, showing weak interactions between the polymers and solvent. Xu et al.[36] also reported that the particle size of the dispersed phase is directly linked to the compatibilization of the blend. These hemicellulose particles indicate their lack of compatibility with the PHB and solvent used.

## 4. Practical applications, limitations, and future directions

Due to environmental concerns over the volume of plastics generated in the 21st century, the use of natural

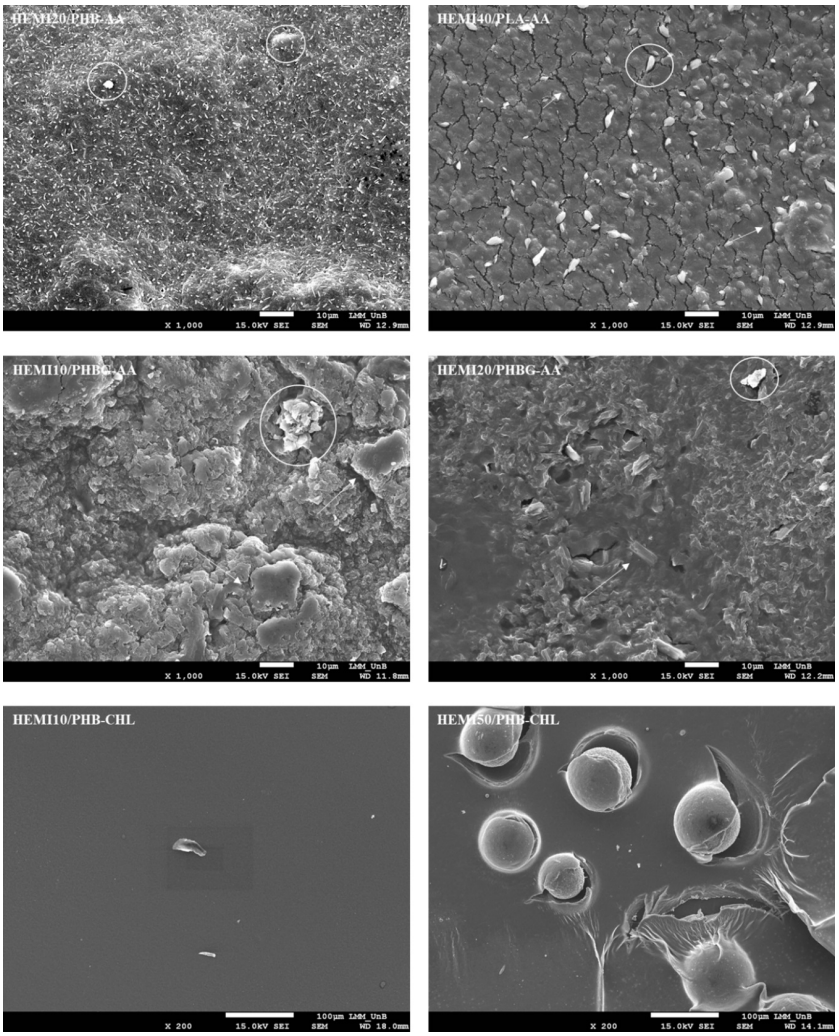


**Figure 7.** SEM images of blends with 1000x magnification for a) Hemi20/PHB-AA, b) Hemi40/PLA-AA, c) Hemi10/PHBG-AA, and d) Hemi20/PHBG-AA and 200x magnification for e) Hemi10/PHB-CHL and f) Hemi10/PHB-CHL.

resources has gained notoriety, mainly from biomass. The present study allowed us to obtain a biodegradable material from hemicellulose by combining it with bio-based materials (PHB and PLA). Thus, promoting new, more sustainable technologies to replace synthetic and fossil-based polymers with more natural ones. The results may also guide planning practice and policymaking concerning bio-derived materials and renewable feedstock proception based on their blending.

The investigation of the effect of different solvents and plasticizer on thermal properties sheds light on the bioplastic market toward surpassing the two main challenges in the development of these blends: incompatibility with different physical and chemical characteristics and processing (due to long side chains that reduce intermolecular interactions and decrease thermal properties)[9,35]. For furthering the knowledge, a complete characterization contemplating mechanical properties is essential and will be explored in future publications. In addition, research on contact angle and water vapor permeability is recommended, among others, for possible applications such as the packaging industry. Moreover, investigations on using compatibilizers, plasticizers or reinforcements are also necessary to increase the miscibility and interaction of these polymers.

In addition, knowing that the focus on sustainable goals permeates industries' responsibility for their processes and disposal of products[45], pursuing strategies and applying systematic environmental approaches[46] are imperative to the commitment toward protecting the environment. Moreover, even though bio-derived polymers are usually considered eco-friendly, the cultivation practices used to grow these feedstocks often have significant environmental impacts[47]. Hence, future research is recommended on advanced sustainability analysis such as life cycle assessment[47].

## 5. Conclusions

The results of the multicriteria analysis demonstrated that AA has a better success rate than CHL as a solvent, corroborating with the visual aspect and thermal behavior

results. Blends of PHB with AA showed an interaction with the hydroxyl groups of hemicellulose as CHL dissolved only its side chain and dispersed its acetyl groups. We also observed that glycerol interacted with hemicellulose and PHB as it reduced the two small peaks of degradation of the blends to one peak. The SEM analysis also observed this interaction of glycerol with the two polymers, where the plasticizer made the film more homogeneous by reducing the particles dispersed on its surface. However, phase separation in the blend occurred with CHL, which indicates their incompatibility. Blends with PLA showed a higher degradation temperature than those with PHB, with more intense peaks indicating its quick degradation. The visual aspect of CHL reveals that phase separation in the blend occurred, which indicates their incompatibility. Thus, AA exhibited a better success rate on MCDA results.

## 6. Acknowledgments

The authors would like to thank CAPES (Coordenação de Aperfeiçoamento de Pessoal de Nível Superior) for providing a scholarship for the first author and DPG/UnB (Decanato de Pós-graduação/University of Brasília), FAPDF (Fundação de Apoio à Pesquisa do Distrito Federal - Projeto 81/2021, Edital 3/2021) and CNPq (Conselho Nacional de Desenvolvimento Científico e Tecnológico) for the financial support for this project.

## 7. References

1. Shao H, Sun H, Yang B, Zhang H, Hu Y. Facile and green preparation of hemicellulose-based film with elevated hydrophobicity via cross-linking with citric acid. RSC Advances. 2019;9:2395-401. http://dx.doi.org/10.1039/C8RA09937E.
2. Silveira EA, Macedo LA, Rousset P, Candelier K, Galvão LGO, Chaves BS, et al. A potassium responsive numerical path to model catalytic torrefaction kinetics. Energy. 2022;239:122208. http://dx.doi.org/10.1016/j.energy.2021.122208.
3. Macedo LA, Silveira EA, Rousset P, Valette J, Commandré J-M. Synergistic effect of biomass potassium content and oxidative atmosphere: impact on torrefaction severity and released condensables. Energy. 2022;254:124472. http://dx.doi.org/10.1016/j.energy.2022.124472.
4. Zhao Y, Sun H, Yang B, Weng Y. Hemicellulose-based film: potential green films for food packaging. Polymers (Basel). 2020;12:1775. http://dx.doi.org/10.3390/polym12081775.
5. Liu H, Chen T, Dong C, Pan X. Biomedical applications of hemicellulose-based hydrogels. Curr Med Chem. 2020;27:4647-59. http://dx.doi.org/10.2174/0929867327666200408115817.
6. Lian Y, Zhang J, Li N, Ping Q. Preparation of hemicellulose-based hydrogel and its application as an adsorbent towards heavy metal ions. BioResources. 2018;13:3208-18. http://dx.doi.org/10.15376/biores.13.2.3208-3218.
7. Huang L, Ma M, Ji X, Choi S, Si C. Recent developments and applications of hemicellulose from wheat straw: a review. Front Bioeng Biotechnol. 2021;9:1-14. http://dx.doi.org/10.3389/fbioe.2021.690773.
8. Godbole S. Preparation and characterization of biodegradable poly-3-hydroxybutyrate–starch blend films. Bioresour Technol. 2003;86:33-7. http://dx.doi.org/10.1016/S0960-8524(02)00110-4.
9. Arrieta M, Samper M, Aldas M, López J. On the use of PLA-PHB blends for sustainable food packaging applications. Materials (Basel). 2017;10:1008. http://dx.doi.org/10.3390/ma10091008.
10. Naser AZ, Deiab I, Darras BM. Poly(lactic acid) (PLA) and polyhydroxyalkanoates (PHAs), green alternatives to petroleum-based plastics: a review. RSC Advances. 2021;11:17151-96. http://dx.doi.org/10.1039/D1RA02390J.
11. Farah S, Anderson DG, Langer R. Physical and mechanical properties of PLA, and their functions in widespread applications: a comprehensive review. Adv Drug Deliv Rev. 2016;107:367-92. http://dx.doi.org/10.1016/j.addr.2016.06.012.
12. Bhiogade A, Kannan M, Devanathan S. Degradation kinetics study of Poly lactic acid(PLA) based biodegradable green composites. Mater Today Proc. 2020;24:806-14. http://dx.doi.org/10.1016/j.matpr.2020.04.389.
13. Seoane IT, Manfredi LB, Cyras VP. Properties and processing relationship of polyhydroxybutyrate and cellulose biocomposites. Procedia Mater Sci. 2015;8:807-13. http://dx.doi.org/10.1016/j.mspro.2015.04.139.
14. Fonseca-García A, Osorio BH, Aguirre-Loredo RY, Calambas HL, Caicedo C. Miscibility study of thermoplastic starch/polylactic acid blends: thermal and superficial properties. Carbohydr Polym. 2022;293:119744. http://dx.doi.org/10.1016/j.carbpol.2022.119744.
15. Sukhanova AA, Murzova AE, Boyandin AN, Kiselev EG, Sukovatyi AG, Kuzmin AP, et al. Poly-3-hydroxybutyrate/chitosan composite films and nonwoven mats. Int J Biol Macromol. 2020;165:2947-56. http://dx.doi.org/10.1016/J.IJBIOMAC.2020.10.177.
16. Awale RJ, Ali FB, Azmi AS, Puad NIM, Anuar H, Hassan A. Enhanced flexibility of biodegradable polylactic acid/starch blends using epoxidized palm oil as plasticizer. Polymers (Basel). 2018;10. http://dx.doi.org/10.3390/polym10090977.
17. Grande R, Pessan LA, Carvalho AJF. Thermoplastic blends of chitosan: A method for the preparation of high thermally stable blends with polyesters. Carbohydr Polym. 2018;191:44-52. http://dx.doi.org/10.1016/j.carbpol.2018.02.087.
18. Anbukarasu P, Sauvageau D, Elias A. Tuning the properties of polyhydroxybutyrate films using acetic acid via solvent casting. Sci Rep. 2016;5:17884. http://dx.doi.org/10.1038/srep17884.
19. Dasan YK, Bhat AH, Ahmad F. Polymer blend of PLA/PHBV based bionanocomposites reinforced with nanocrystalline cellulose for potential application as packaging material. Carbohydr Polym. 2017;157:1323-32. http://dx.doi.org/10.1016/j.carbpol.2016.11.012.
20. Nerkar M, Ramsay JA, Ramsay BA, Vasileiou AA, Kontopoulou M. Improvements in the melt and solid-state properties of poly(lactic acid), poly-3-hydroxyoctanoate and their blends through reactive modification. Polymer (Guildf). 2015;64:51-61. http://dx.doi.org/10.1016/j.polymer.2015.03.015.
21. Geeti DK, Niranjan K. Environmentally benign bio-based waterborne polyesters: synthesis, thermal- and bio-degradation studies. Prog Org Coat. 2019;127:419-28. http://dx.doi.org/10.1016/j.porgcoat.2018.11.034.
22. Xu J, Xia R, Zheng L, Yuan T, Sun R. Plasticized hemicelluloses/chitosan-based edible films reinforced by cellulose nanofiber with enhanced mechanical properties. Carbohydr Polym. 2019;224:115164. http://dx.doi.org/10.1016/j.carbpol.2019.115164.
23. Kataoka LFMS, Hidalgo Falla MDP, Luz SM. The influence of potassium hydroxide concentration and reaction time on the extraction cellulosic jute fibers. J Nat Fibers. 2021;19(13):6889-901. http://dx.doi.org/10.1080/15440478.2021.1934934.
24. Dalla Libera V Jr, Leão RM, Franco Steier V, da Luz SM. Influence of cure agent, treatment and fibre content on the thermal behaviour of a curaua/epoxy prepreg. Plast Rubber Compos. 2020;49:214-21. http://dx.doi.org/10.1080/14658011.2020.1729658.
25. Silveira EA, Luz S, Santanna MS, Leão RM, Rousset P, Pires AC. Thermal upgrading of sustainable woody material: experimental and numerical torrefaction assessment. In: 28th European Biomass Conference and Exhibition; 2020; Florence.

Proceedings. Florence: ETA-Florence Renewable Energies; 2020. p. 694-8. https://doi.org/10.5071/28thEUBCE2020-3CV.2.5.

26. Evaristo RBW, Ferreira R, Petrocchi Rodrigues J, Sabino Rodrigues J, Ghesti GF, Silveira EA, et al. Multiparameter-analysis of CO2/steam-enhanced gasification and pyrolysis for syngas and biochar production from low-cost feedstock. Energy Convers Manag X. 2021;12:100138. http://dx.doi.org/10.1016/j.ecmx.2021.100138.
27. Ghesti GF, Silveira EA, Guimarães MG, Evaristo RBW, Costa M. Towards a sustainable waste-to-energy pathway to pequi biomass residues: biochar, syngas, and biodiesel analysis. Waste Manag. 2022;143:144-56. http://dx.doi.org/10.1016/j.wasman.2022.02.022.
28. Silveira EA, Chaves BS, Macedo LA, Ghesti GF, Evaristo RBW, Cruz Lamas G, et al. A hybrid optimization approach towards energy recovery from torrefied waste blends. SSRN Electron J 2022. https://doi.org/10.2139/ssrn.4217358.
29. Lamas GC, Costa FC, Santanna MSS, Chaves B, Galvão LGO, Macedo L, et al. Steam-enhanced gasification of a hybrid blend composed of municipal solid waste and torrefied biomass. In 30th European Biomass Conference and Exhibition; 2022; Florence. Proceedings. Florence: ETA-Florence Renewable Energies; 2022. p. 9-12. https://doi.org/10.5071/30thEUBCE2022-1CV.2.2.
30. Deb K. Multi-objective optimisation using evolutionary algorithms: an introduction. In: Wang L, Ng A, Deb K, editors. Multi-objective evolutionary optimisation for product design and manufacturing. London: Springer; 2011. p. 3-34. https://doi.org/10.1007/978-0-85729-652-8_1.
31. Wang X, Liow SS, Wu Q, Li C, Owh C, Li Z, et al. Codelivery for paclitaxel and Bcl-2 conversion gene by PHB-PDMAEMA amphiphilic cationic copolymer for effective drug resistant cancer therapy. Macromol Biosci. 2017;17:1700186. http://dx.doi.org/10.1002/mabi.201700186.
32. Roldi-Oliveira M, Diniz LM, Elias AL, Luz SM. Hemicellulose films from curaua fibers (ananas erectifolius): extraction and thermal and mechanical characterization. Polymers (Basel). 2022;14:2999. http://dx.doi.org/10.3390/polym14152999.
33. Samanta AK, Mukhopadhyay A, Ghosh SK. Processing of jute fibres and its applications. In: Kozłowski RM, Mackiewicz-Talarczyk M, editors. Handbook of natural fibres. Sawston, Reino Unido: Woodhead Publishing; 2020. p. 49-120. https://doi.org/10.1016/B978-0-12-818782-1.00002-X.
34. Mendes FRS, Bastos MSR, Mendes LG, Silva ARA, Sousa FD, Monteiro-Moreira ACO, et al. Preparation and evaluation of hemicellulose films and their blends. Food Hydrocoll. 2017;70:181-90. https://doi.org/10.1016/j.foodhyd.2017.03.037.
35. Quispe MM, Lopez OV, Boina DA, Stumbé J-F, Villar MA. Glycerol-based additives of poly(3-hydroxybutyrate) films. Polym Test. 2021;93:107005. http://dx.doi.org/10.1016/j.polymertesting.2020.107005.
36. Xu W, Pranovich A, Uppstu P, Wang X, Kronlund D, Hemming J, et al. Novel biorenewable composite of wood polysaccharide and polylactic acid for three dimensional printing. Carbohydr Polym. 2018;187:51-8. http://dx.doi.org/10.1016/j.carbpol.2018.01.069.
37. Nechita P, Mirela R, Ciolacu F. Xylan hemicellulose: a renewable material with potential properties for food packaging applications. Sustainability. 2021;13:13504. http://dx.doi.org/10.3390/su132413504.
38. Arrieta MP, López J, Hernández A, Rayón E. Ternary PLA–PHB–Limonene blends intended for biodegradable food packaging applications. Eur Polym J. 2014;50:255-70. http://dx.doi.org/10.1016/j.eurpolymj.2013.11.009.
39. Mendes FRS, Bastos MSR, Mendes LG, Silva ARA, Sousa FD, Monteiro-Moreira ACO, et al. Preparation and evaluation of hemicellulose films and their blends. Food Hydrocoll. 2017;70:181-90. http://dx.doi.org/10.1016/j.foodhyd.2017.03.037.
40. Silveira EA, Luz SM, Leão RM, Rousset P, Caldeira-Pires A. Numerical modeling and experimental assessment of sustainable woody biomass torrefaction via coupled TG-FTIR. Biomass Bioenergy. 2021;146:105981. http://dx.doi.org/10.1016/j.biombioe.2021.105981.
41. Silveira EA, Santanna MS, Barbosa Souto NP, Lamas GC, Galvão LGO, Luz SM, et al. Urban lignocellulosic waste as biofuel: thermal improvement and torrefaction kinetics. J Therm Anal Calorim. 2023;148:197-212. http://dx.doi.org/10.1007/s10973-022-11515-0.
42. Jin C, Zhang X, Geng Z, Pang X, Wang X, Ji J, et al. Effects of various co-solvents on the solubility between blends of soybean oil with either methanol or ethanol. Fuel. 2019;244:461-71. http://dx.doi.org/10.1016/j.fuel.2019.01.187.
43. Lopera-Valle A, Caputo JV, Leão R, Sauvageau D, Luz SM, Elias A. Influence of epoxidized Canola Oil (eCO) and Cellulose Nanocrystals (CNCs) on the mechanical and thermal properties of polyhydroxybutyrate (PHB)-Poly(lactic acid) (PLA) blends. Polymers (Basel). 2019;11:933. http://dx.doi.org/10.3390/polym11060933.
44. Azeredo HMC, Kontou-Vrettou C, Moates GK, Wellner N, Cross K, Pereira PHF, et al. Wheat straw hemicellulose films as affected by citric acid. Food Hydrocoll. 2015;50:1-6. http://dx.doi.org/10.1016/j.foodhyd.2015.04.005.
45. Deutsch L, Lamas GC, Pereira TS, Silveira EA, Caldeira-Pires A. Life cycle and risk assessment of vinasse storage dams: a Brazilian sugar-energy refinery analysis. Sustain Futur. 2022;4:100083. http://dx.doi.org/10.1016/j.sftr.2022.100083.
46. Silveira EA, Caldeira-Pires A, Luz SM, Silveira CM. Mass and energy allocation method analysis for an oil refinery characterization using multi-scale modeling. Int J Life Cycle Assess. 2017;22:1815-22. https://doi.org/10.1007/s11367-017-1369-9.
47. Yates MR, Barlow CY. Life cycle assessments of biodegradable, commercial biopolymers - A critical review. Resour Conserv Recycling. 2013;78:54-66. http://dx.doi.org/10.1016/j.resconrec.2013.06.010.